Review and Comparison of Methods to Model Ship Hull Roughness

Citation for the original published paper (version of record):
Andersson, J., Oliveira, D., Yeginbayeva, I. et al (2020). Review and Comparison of Methods to Model Ship Hull Roughness. Applied Ocean Research, 99.
http://dx.doi.org/10.1016/j.apor.2020.102119

Applied Ocean Research 99 (2020) 102119

Contents lists available at ScienceDirect

Applied Ocean Research

journal homepage: www.elsevier.com/locate/apor

Review and comparison of methods to model ship hull roughness

Jennie Andersson*,[a], Dinis Reis Oliveira[a], Irma Yeginbayeva[b], Michael Leer-Andersen[c], Rickard E. Bensow[a]

[a] Chalmers University of Technology, Department of Mechanics and Maritime Sciences, 412 96 Göteborg, Sweden
[b] Jotun A/S, Rosenvolds gate 19, 3211 Sandefjord, Norway
[c] SSPA Sweden AB, Chalmers Tvärgata 10, 400 22 Göteborg, Sweden

ARTICLE INFO

Keywords:
Hull roughness
Roughness function
Ship-scale CFD
KVLCC2
Fouling

ABSTRACT

There is a large body of research available focusing on how ship hull conditions, including various hull coatings, coating defects, and biofouling, influence the boundary layer, and hence resistance and wake field of a ship. Despite this there seems to be little consensus or established best practice within the ship design community on how to model hull roughness for ship-scale CFD. This study reviews and compares proposed methods to model hull roughness, to support its use in the ship design community. The impact of various types of roughness on additional resistance and wake fields are computed and presented for the well-established test case KVLCC2. The surfaces included in the review are divided into three groups: 1) high quality, newly painted surfaces, 2) surfaces with different extent of poor paint application and/or hull coating damages; and 3) surfaces covered with light slime layers. The review shows the use of a variety of roughness functions, both Colebrook-type and inflectional with three distinct flow regimes, as well as a variety of strategies to obtain the roughness length scales. We do not observe any convergence within the research community towards specific roughness functions or methods to obtain the roughness length scales. The comparison using KVLCC2 clearly illustrates that disparities in surface texture cause large differences in additional resistance, and consequently no strong correlation to a single parameter, e.g. AHR (Average Hull Roughness). This implies that, to be able to select a suitable hull roughness model for a CFD-setup, more details of the surface characteristics are required, such as hydrodynamic characterization of hull coating and expected fouling.

1. Introduction

Within ship design, model-scale testing in towing tanks and associated scaling procedures [1] has traditionally been the main tool for performance prediction for use in contractual agreements between suppliers and owners. In parallel, and as a complement to model testing, the use of Computational Fluid Dynamics (CFD) has also become an important part of every ship design process. The focus of CFD validation work conducted within the field has mainly been on model-scale CFD, such as the workshop series in Numerical Ship Hydrodynamics, firstly organized in 1980 and the latest held in Gothenburg 2010 [2] and Tokyo 2015 [3]. The focus of validation work on model-scale CFD is a natural consequence of the lack of detailed flow data to use for validation in ship-scale, and also the often uncertain boundary conditions, environmental conditions, ship geometry etc., associated with such data. However, to be able to fully complement the model-scale testing and associated scaling procedures with CFD, it is necessary to model the ship in its actual size. This in general implies large differences in Reynolds numbers, from around 10^6 in model-scale to about 10^8–10^9 in ship-scale, with significant effects on the boundary layer development and wake formation. Another important difference between model and ship-scale is that the hull surface generally can be assumed as hydraulically smooth in model-scale, which is seldom the case for the actual vessel. Surface roughness not only influences the resistance of the ship, it also alters the entire boundary layer development and wake formation, which will have an effect on the propulsive performance and optimal propulsion system design.

Historically, there is a large body of research conducted focusing on how the hull conditions, including various hull coatings, coating defects, corrosion and biofouling, influence the resistance of a ship, for instance summarized by Townsin [4], referring back to work conducted in the 19th century. Studies have also been conducted on how a rough surface influences the boundary layer, an area pioneered by Nikuradse [5] and Colebrook [6] for rough pipes. For ship design, these studies have been complemented with work specifically focusing on how the boundary layer is affected by various hull conditions, from clean hull

* Corresponding author.
E-mail address: jennie.andersson@chalmers.se (J. Andersson).

https://doi.org/10.1016/j.apor.2020.102119
Received 23 October 2019; Received in revised form 13 February 2020; Accepted 9 March 2020
Available online 30 April 2020

coatings to severe biofouling [7,8]. This research field was strongly influenced by the ban on TBT (tributyltin) biocides from hull coatings in the beginning of the 21st century, and development of more environmentally-friendly alternatives to deter fouling, such as self-polishing copper-based antifouling and non-biocidal foul-release coatings [9].

Despite all research conducted on the hydrodynamic effects of various hull conditions, it seems there is little consensus or established best practice within the ship design community on how to model hull roughness for ship-scale CFD. This was clearly noticed in the 2016 Workshop on Ship Scale Hydrodynamic Computer Simulations [10], where only three participants out of 17 included modelling of hull roughness. A complicating factor is that relevant roughness characteristics of the ship hull surface are often unknown to the CFD-user, and if it is, the only available data is $R_{t,50}$ (the maximum peak-to-trough height taken over a 50-mm sample length), the most common measure of hull roughness, also known as the Average Hull Roughness (AHR) when it is combined to one single parameter through averaging several measurements on the hull. The AHR is obtained according to standardized procedures and is not equivalent to the roughness length scales required as input for surface roughness models available in general CFD software.

The objective of this study is to review and compare different methods to model hull roughness, which all could be used as input to ship-scale CFD. The study is limited to relatively clean hull surfaces, ranging from high quality newly painted hulls to different extent of poor paint application and/or hull coating damages and light slime layers. More severe biofouling, such as heavy slime layers, weed (filamentous alga) and calcareous fouling are excluded.

This paper is structured as follows: Section 2 and 3 includes a review of methods to model hull roughness. To compare these methods in terms of effects on hull resistance and wake field they will all be applied on the freely available hull shape KVLCC2, which will be described in Section 4. The flow solver, computational domain, boundary conditions, and computational grids are described in Section 5. The comparison and associated discussions are included in Section 6, and the conclusions are summarized in Section 7.

2. Approaches to model effects of surface roughness

The most common approach in literature to describe the hydrodynamic effects of ship hull surface roughness is through a downward velocity shift in the turbulent boundary layer (logarithmic overlap layer):

$$U^+ = \frac{1}{\kappa}\ln(y^+) + B - \Delta U^+, \tag{1}$$

where κ is the von Karman constant and B is the constant for smooth-wall log-law intercept. ΔU^+ is the roughness function, dependent on the roughness Reynolds number k^+, defined as $k^+ = ku^*/\nu$, where k is the roughness length scale, u^* the friction velocity and ν the kinematic viscosity. The most commonly-used roughness length scale is the equivalent sand grain roughness height, since the first experiments within the area were conducted on surfaces covered with densely packed sand. This length scale is a hydraulic parameter that must be determined experimentally [11] and may depend on several geometrical parameters of the surface.

Various roughness functions, $\Delta U^+ = f(k^+)$, are suggested in the literature. The common roughness functions for hull surfaces can generally be divided into two groups, inflectional-behaviour functions, with three distinct flow regimes, and single expression functions, the latter commonly referred to as Colebrook/Grigson-type. The roughness functions by Cebeci and Bradshaw [12] and Schultz and Flack [8,13] belongs to the first group and both follow the traditional Nikuradse [5] roughness function shape, including the three regimes that have been termed hydraulically smooth, transitionally rough and fully rough. In the hydraulically smooth regime the surface roughness is smooth enough so that any perturbations caused by roughness elements are completely damped out by viscosity, resulting in that $\Delta U^+ = 0$. At higher k^+ the surface roughness elements start to produce pressure drag, influencing the surface frictional drag and roughness function and at a certain point it is considered that the drag on the surface is entirely due to the pressure drag on the roughness elements, which is referred to as the fully rough flow regime. The limits between the different flow regimes are considered, at least to some extent, to depend on the roughness type [14]. These roughness functions can generally be written in the form:

$$\Delta U^+ = \begin{cases} 0 & k^+ \le k^+_{smooth} \\ \frac{1}{\kappa}\ln(C_s k^+)\cdot\sin\left(\frac{\pi}{2}\frac{\ln(k^+/k^+_{smooth})}{\ln(k^+_{rough}/k^+_{smooth})}\right) & k^+_{smooth} < k^+ \le k^+_{rough} \\ \frac{1}{\kappa}\ln(C_s k^+) & k^+ > k^+_{rough} \end{cases} \tag{2}$$

For Cebeci and Bradshaw [12] the constants are given as: $k^+_{smooth} = 2.25$, $k^+_{rough} = 90$ and $C_s = 0.253$ or 0.5, where the first value corresponds to the traditional Nikuradse roughness function [5]. Demirel et al. [8] fitted the roughness function proposed by Schultz and Flack [13] to this roughness function shape with the constants $k^+_{smooth} = 3$, $k^+_{rough} = 15$ and $C_s = 0.26$.

The second group of roughness functions, originally suggested by Colebrook [6], and later adopted by Grigson [15], is based on a single expression to describe $\Delta U^+ = f(k^+)$, most commonly used in the form:

$$\Delta U^+ = \frac{1}{\kappa}\ln(1 + k^+). \tag{3}$$

It has been lively debated, as for instance shown in [16], on if the three distinct regimes or a single expression like Eq. (3) is most suitable to describe a typical ship hull surface, without yet reaching any consensus. The roughness functions mentioned above are the ones included in this review and these are also illustrated graphically in Fig. 1 in the section below.

It should also be mentioned that, besides roughness functions, there are two other alternative methods to model hull roughness in CFD: 1) a Low-Reynolds number turbulence model with modified boundary conditions, and 2) geometrically resolving the rough surface geometry. Regarding the first alternative, a common modification of a Low-Reynolds number turbulence model to account for roughness is suggested by Wilcox [17], which for instance has been applied in [18]. All studies known to the authors that focus on how the characteristics of various ship hull surfaces should be expressed in terms of the roughness length scale relate the surface impact on the flow using a roughness functions, $\Delta U^+ = f(k^+)$. Therefore, if applying a Low-Reynolds number turbulence model, it is critical to ensure that the Low-Reynolds number roughness model's impact on the boundary layer is replicating the behavior of the roughness function associated with the method to obtain the roughness length scale, see for instance [19]. A further complication with the application of a Low-Reynolds number turbulence model is that it may be computationally expensive; the near-wall-cell thickness required at ship-scale Reynolds numbers most often also results in a reduced cell size in x^+- and z^+-directions to maintain an acceptable grid quality, with a large increase in grid count as a consequence. As for the second alternative approach, i.e. to simulate the flow over a geometrically-resolved rough surface, it is not sufficient with a Reynolds-Average Navier-Stokes (RANS) model, and a DNS (Direct Numerical Simulation) approach would be required, which is currently unfeasible for ship-scale CFD. Concluding this, due to the limitations of the two alternative methods to model hull roughness this review will focus on methods to model hull roughness based on various roughness functions and associated roughness length scales.

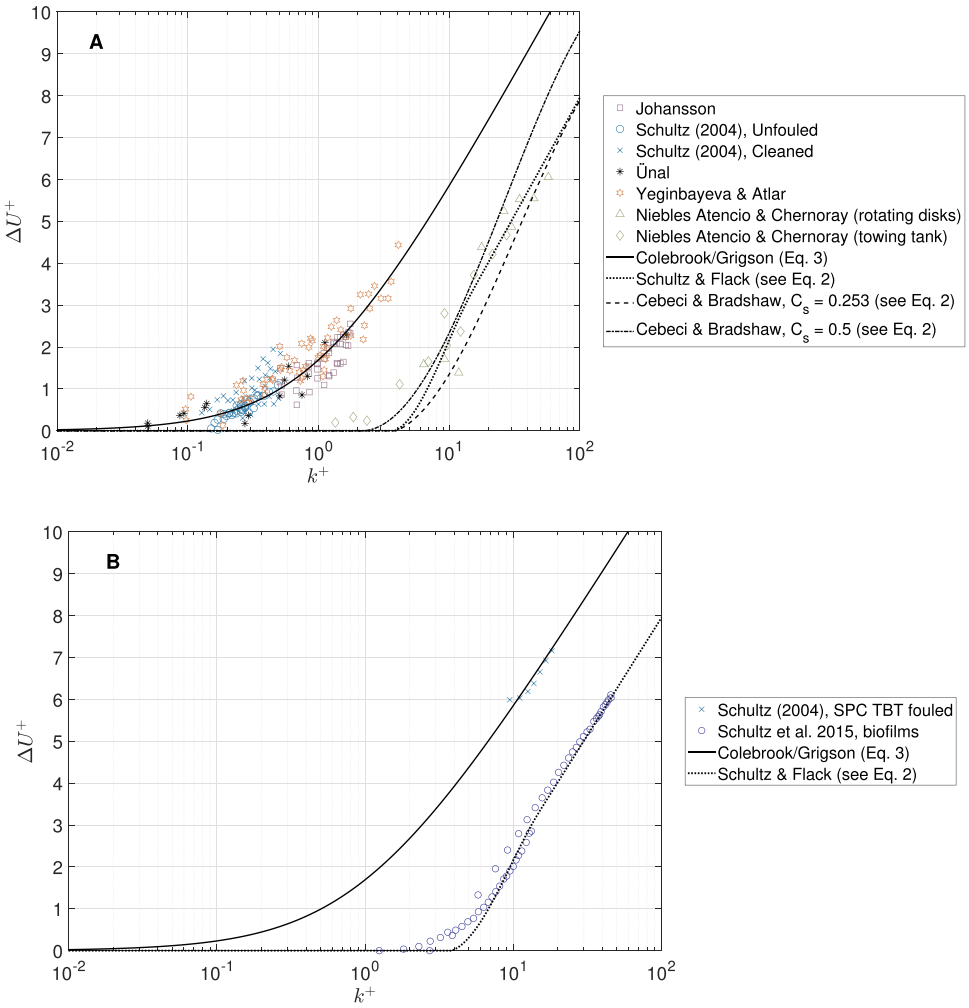

Fig. 1. Roughness function ΔU^+ vs. roughness Reynolds number k^+, including original data from selected studies listed in Table 1 for hull coatings (A) and thin slime layers (B).

3. Scope of current study

A summary of earlier work conducted within the field is made by the 19th ITTC [16], at that time most of the work was focusing on self polishing copolymer (SPC) TBT systems which are banned today due to their adverse environmental impacts. A pioneer in the studies of more modern hull coatings was Candries [20], who conducted experimental studies and compared it with other available surface data, however without presenting a model for surface roughness based on the coatings studied.

The hull surface models included in this review and comparison are summarized in Table 1 and Fig. 1. The review is limited to models developed specifically for various conditions of the hull surface. Further it is also limited to those studies where it is possible to obtain the roughness length scale for specific surfaces (typical hull conditions) from the information provided in each study. This is important since CFD users most often do not possess detailed hull surface parameters such as roughness amplitudes, skewness, slope angle and/or wave length of the specific ship hull surface, often required to obtain the roughness length scale.

As listed in Table 1, previous experimental data has been obtained from different facilities, such as towing tank, cavitation tunnel, channel flow and rotating disk tests (the CFD data in [26] was not sufficient for deriving a roughness function and roughness length scale). The experimental work by Schultz [22] was conducted at the US Naval Academy Hydromechanics Laboratory in Annapolis. The research conducted by both Ünal [23] and Yeginbayeva and Atlar [25] is based on experiments in the Emerson cavitation tunnel of Newcastle University, with hull coatings supplied by International Paint Ltd. (a division of Akzo-Nobel). Both Leer-Andersen et al. [24], conducting their experiments in the SSPA towing tank, and Niebles Atencio and Chernoray [26], using towing tank tests performed at MARINTEK [27], were supplied by paints from Jotun A/S. Also Johansson [21] conducted his experiments at SSPA, however in a cavitation tunnel. It can be noted that all experiments are conducted on flat plates without any pressure gradients in the flow, unlike the flow around curved ship hull surfaces. The Reynolds number ranges supplied in Table 1, based on plate length or distance from leading edge to measurement section, cannot really be compared directly, since turbulence is triggered prior to the rough plate for the experiments by Ünal [23], Leer-Andersen et al. [24] and Yeginbayeva and Atlar [25]. For the towing tank tests used by Niebles Atencio and Chernoray [27], a smooth 4 m long leading plate was used to ensure turbulent boundary layer on the test plate. To be able to compare the different tests in terms of hydrodynamic conditions it would have been better to use Reynolds numbers based on boundary layer thickness, or else based on momentum thickness. However, such values were not provided in all studies of Table 1.

The studies included in the review and listed in Table 1 include various hull surface conditions, from which some surfaces were selected for comparison according to the delimitation of the study, i.e relatively clean surfaces, ranging from high quality newly painted, to different extent of poor paint application and/or coating damages and light slime

Table 1
Summary of hull surface models included in the review.

Publication	Data source	Reynolds number	Type of surfaces	Roughness function	Method to obtain roughness length scale (k)
Johansson [21]	Cavitation tunnel tests	Unknown	Unfouled and fouled	Colebrook/Grigson, Eq. (3)	*AHR/C, C* specific for each surface
Schultz [22]	Towing tank tests	$2.8{\cdot}10^6$ – $5.5{\cdot}10^6$	Unfouled, fouled and cleaned	Colebrook/Grigson, Eq. (3)	$0.17 \cdot R_a$ *(unfouled, cleaned)* $0.11 \cdot$ *biofilm thickness (slime)*
Schultz) [7]	Data from [22]	$2.8{\cdot}10^6$ – $5.5{\cdot}10^6$	Unfouled, fouled and cleaned	Schultz and Flack [8,13] see Eq. (2)	Specific values for 6 surfaces
Ünal [23]	Cavitation tunnel tests	$5.5{\cdot}10^6$ – $1.6{\cdot}10^7$	Unfouled	Colebrook/Grigson, Eq. (3)	$15.77{\cdot}R_q(1 + Sk)^{0.862}/Sd_4$
Leer-Andersen et al. [24]	Towing tank tests	$1.3{\cdot}10^7$ – $3.1{\cdot}10^7$	Unfouled, fouled, cleaned and with mimicked coating damages	Colebrook/Grigson, Eq. (3)	*AHR/C, C* specific for each surface
Yeginbayeva and Atlar [25]	Cavitation tunnel tests	$5.6{\cdot}10^6$ – $1.7{\cdot}10^7$	Unfouled and with mimicked hull roughness	Colebrook/Grigson, Eq. (3)	$0.6 \cdot R_a$
Niebles Atencio and Chernoray [26]	Towing tank and rotating disk tests, CFD	$1.4{\cdot}10^6$ – $9.0{\cdot}10^7$	Unfouled and with mimicked hull roughness	Cebeci and Bradshaw [12] see Eq. (2)	R_q

layers. The roughness functions and methods to obtain the roughness length scale listed in Table 1 are valid for the surfaces selected for comparison in this review, but not necessary for all surface conditions included in each original study.

Prior to discussing the method to obtain the roughness length scale k, some notes need to be made about how the surface roughness characteristics, i.e. parameters such as roughness amplitudes, skewness, slope angle and wave length, have been obtained. Detailed surface analyses using laser/optical profilometers have been used within all studies except from Johansson [21] and Leer-Andersen et al. [24]. The focus of the work conducted by Ünal [23] is to a large extent how different data treatment methods of the raw data from a laser profilometer influence the possibility to correlate the roughness characteristics with a roughness function. Different combinations of sampling lengths, moving average filtering with various cut-off lengths (i.e. the sampling length used for evaluation of roughness parameters) and sampling length averaging were investigated. A large impact of the roughness parameter calculation methods on the roughness function correlations was demonstrated, with different impacts on different surface topographies. The conclusion drawn was that an elimination of waviness from the primary profile through moving average filtering was necessary, and the best results were obtained for a short (81-points) moving-average low-pass filter, i.e. a relatively short cut-off length. Candries [20] has previously also found that effective cut-off lengths for hydrodynamic purposes lies between 2.5 mm and 5 mm for coated surfaces. It is clear that the surface texture parameters are most sensitive to the short wavelength cut-off, while the roughness amplitude parameters are more sensitive to the long wavelength cut-off.

Surface waviness has been removed using a 5 mm long wavelength filtering (Ünal [23] and Yeginbayeva and Atlar [25]) and 8 mm long wavelength filtering (Niebles Atencio and Chernoray [26]]), respectively, whereas the data treatment by Schultz [22] is unknown. Based on the study by Ünal [23] it is clear that the data filtering may be the reason behind differences in the methods to obtain the roughness length scale, and it may also explain why certain studies do not succeed in matching their surface roughness characteristics with previously published methods. Further, in all studies except from Ünal [23] the surfaces have also been characterized using a standard stylus-probe hull roughness analyzer.

As discussed above, there is no common agreement on which type of roughness function to apply for typical ship hull surfaces. Amongst the studies listed in Table 1, no strong arguments in favour of a specific type of roughness function are present. Schultz [7] claim that his experimental data agree reasonably well with Schultz and Flack [8,13] (see Eq. (2)). Ünal [23] and Yeginbayeva and Atlar [25] motivate the selection of a Colebrook/Grigson (Eq. (3)) type of roughness function by that it is broadly accepted for naturally occurring engineering surfaces and commonly used for marine coatings. Ünal [23] did not note an inflectional-behaviour roughness function based on his data, but also admits the lack of data in the transitionally rough flow regime to fully justify this behaviour. The use of the Cebeci and Bradshaw [12] (see Eq. (2)) roughness function is motivated by its availability in commercial CFD software [26].

Neither is there any common agreement on whether one surface parameter is enough, or else on how many parameters are required to characterize a surface and obtain a roughness length scale to be used for the correlation with the roughness function. Many agree that theoretically at least two surface parameters, one based on roughness height and another one on the texture, should be used to characterize a surface in terms of a roughness length scale k. However, several other studies concludes that one surface parameter is enough to describe surfaces with similar textures. Schultz [7] does not specify in detail how the roughness length scales have been obtained. Ünal [23] uses a correlation including several surface roughness parameters: root-mean-square deviation of the surface (R_q), skewness (Sk) and mean spacing between the zero-crossings (Sd_4). The model used by Johansson [21] and Leer-

Andersen et al. [24] requires an efficiency constant C, specific for each surface, which is a strategy to account for the surface texture (these constants are indirectly available through an open database [28], however not yet published for Leer-Andersen et al. [24], but have been made available specifically for this comparative review). In the original studies, the constant C is included in the roughness function, which is equivalent to incorporate it in the roughness length scale. Yeginbayeva and Atlar [25] presents three different suggestions on how to obtain the roughness length scale, but since the correlation was better with the methods using only one single parameter, only one of these is applied within this comparison. For unfouled coatings, both Schultz [22] and Yeginbayeva and Atlar [25] use multiples of R_a, with different constants, which clearly illustrates the dependency on either texture or filtering of laser profilometer raw data. Another method is used by Niebles Atencio and Chernoray [26] where a constant, C_S, in the roughness function is varied dependent on the surface. However, it should be noted that most of these correlations still rely on data showing quite some scatter, which is clearly seen in Fig. 1A, where the accordance between roughness Reynolds number for experimental data and roughness function is rather weak. It is also worth to make an additional remark on that there are large differences in the relationship between ΔU^+ and k^+ between the different roughness functions, as clearly illustrated in Fig. 1. This implies that a certain method to obtain the roughness length scale is only suitable to use together with the roughness function it was developed for.

To facilitate the comparison the different surfaces are divided into three groups: the first one containing surfaces described as high quality newly painted hulls in Table 2, the second one including surfaces with different extent of poor paint application and/or hull coating damages in Table 3, and the third focusing on surfaces covered with light slime layers in Table 4. Note that only a selection of surfaces from the studies listed in Table 1 are included in this review. In the last column of Tables 2 and 3 the ratio between AHR and the roughness length scale are provided to illustrate the wide range of values obtained for this ratio, even when using the same roughness function.

For the data in Table 2 almost all studies specify that the coating has been applied according to instructions from paint manufacturers using an airless spray technique. It is however expected to be a general problem that the paint application carried out in laboratory settings allows a much smoother paint application, due to better control of environmental factors and application technique, compared to what is expected on an actual ship hull. The AHR of a new ship lies between 75–125 μm [25], which is above or in the upper range of the values listed in Table 2 except from Schultz [7].

In Table 3 several surfaces were generated in laboratory settings to mimic actual hull roughness experienced on ships. In the study by Yeginbayeva and Atlar [25] the mimicked roughness is claimed to be based on experience of International Paint Ltd and their analysis of a dataset of 845 hull roughness surveys, however the artificial roughness is simply created by inclusion of sand grit in the underlying anticorrosive coating. The rough surfaces studied by Niebles Atencio and Chernoray [26,27] were created through poor paint application, using overspraying and dry spraying. Additionally, two other surfaces, the first from Leer-Andersen et al. [24] and the second from Schultz [22], were created through exposure to fouling and thereafter cleaned.

The most challenging cases to characterize within this comparative review is certainly the surfaces covered with thin slime layers, included in Table 4. Several studies on slime layers (i.e. biofilms) are conducted without the possibility to propose a model for these surfaces, see for instance [29,30]. Schultz et al. [30] suggests the roughness length scale $k = 0.055 \cdot k_{bf} \sqrt{\%\, biofilm\ coverage}$, where k_{bf} is the thickness of the biofilm, however leaving out the suggestion of an equation for the roughness function. Slime layers are difficult to characterize due to their non-uniformity and also difficult to conduct measurements on, since they most often are partially removed during the experiments. Also, it is not possible to measure th e AHR for a slime layer using the standardized stylus-probe procedure, and a value has therefore been estimated by Leer-Andersen et al. [24] since it is required by their model. Biofilm thickness is typically estimated in air, using a wet film thickness gauge [22,29].

To show how the differences in roughness function and roughness length scales influence hull resistance and wake field, the surfaces listed above are applied on the KVLCC2 hull.

4. Ship hull used for comparison of hull roughness models - KVLCC2

The KVLCC2 hull was designed as a test case for CFD and a full-scale ship has never been built. In spite of this, the KVLCC2 hull is modelled in full scale within the present paper, given that hull surface roughness only plays a significant role at ship-scale Reynolds numbers. The original KVLCC2 hull designed around 1997 is selected, which is the one used and described for instance in the 2010 Workshop in Ship Hydrodynamics [2]. A side view of the hull is shown in Fig. 2 and the main particulars are provided in Table 5. The design speed of the vessel corresponds to a Reynolds number (Re) of $1.9 \cdot 10^9$ (Froude number (Fn) = 0.142).

5. CFD Method

The commercial CFD software STAR-CCM+ v12.06 [31], a finite volume method solver, is employed to solve the RANS equations. STAR-CCM+ is a general purpose CFD code used for a wide variety of applications. As applied within this study it solves the conservation equations for momentum, mass, and turbulence quantities using a segregated solver based on the SIMPLE-algorithm. A second order upwind discretization scheme in space is used. Turbulence is modelled using SST k-ω [32,33] with quadratic constitutive relations [34] and curvature correction [31,35], a model which has shown good agreement with model scale tests. More commonly used within the ship design community may be the standard SST k-ω turbulence model, it should therefore be noted that the differences between the two models

Table 2
Selected high quality, newly painted surfaces.

Publication	Description	AHR [μm]	Roughness function	Roughness length scale, k [μm]	AHR/k
Yeginbayeva and Atlar [25]	Foul-release coating	~ 40	Colebrook/Grigson, Eq. (3)	1.2	33
Yeginbayeva and Atlar [25]	Controlled-depletion polymer (CDP)	~ 50	Colebrook/Grigson, Eq. (3)	4.8	10
Niebles Atencio and Chernoray [26]	Optimal newly-built ship, epoxy primer	56	Cebeci and Bradshaw [12] see Eq. (2), $C_s = 0.5$	8.5	7
Leer-Andersen et al. [24]	Self-polishing silyl acrylate	~ 65	Colebrook/Grigson, Eq. (3)	0.02	2900
Leer-Andersen et al. [24]	Traditional anti-fouling	~ 65	Colebrook/Grigson, Eq. (3)	0.8	82
Schultz [22]	Silicone (1)	66	Colebrook/Grigson, Eq. (3)	2.04	32
Schultz [22]	SPC Copper	97	Colebrook/Grigson, Eq. (3)	2.55	38
Schultz [7]	Typical as applied AF coating	150	Schultz and Flack [8,13] see Eq. (2)	30	5
Ünal [23]	Foul-release coating	-	Colebrook/Grigson, Eq. (3)	0.7	N/A

Table 3
Selected surfaces with different extent of poor paint application and/or hull coating damages.

Publication	Description	AHR [μm]	Roughness function	Roughness length scale, k [μm]	AHR/k
Leer-Andersen et al. [24]	Cleaned with high pressure water	~ 110	Colebrook/Grigson, Eq. (3)	2.89	38
Leer-Andersen et al. [24]	Poorly applied anti-fouling (dry-spray)	~130	Colebrook/Grigson, Eq. (3)	3.19	41
Johansson [21]	Badly painted surface	132	Colebrook/Grigson, Eq. (3)	5.04	26
Schultz [22]	SPC TBT, after cleaning	135	Colebrook/Grigson, Eq. (3)	3.74	36
Niebles Atencio and Chernoray [26]	Poorly applied coating, epoxy primer	214	Cebeci and Bradshaw [12] see Eq. (2), C_s = 0.5	41	5
Yeginbayeva and Atlar [25]	Foul-release coating, low roughness	~220	Colebrook/Grigson, Eq. (3)	4.49	49
Yeginbayeva and Atlar [25]	Linear-polishing polymer (LPP)/ Controlled-depletion polymer (CDP), low roughness	~250	Colebrook/Grigson, Eq. (3)	11.70	21
Yeginbayeva and Atlar [25]	Foul-release coating, high roughness	~250	Colebrook/Grigson, Eq. (3)	5.10	49
Schultz [7]	Deteriorated coating (or light slime)	300	Schultz and Flack [8,13] see Eq. (2)	100	3
Yeginbayeva and Atlar [25]	Linear-polishing polymer (LPP)/ Controlled-depletion polymer (CDP), high roughness	~320	Colebrook/Grigson, Eq. (3)	14.98	21
Niebles Atencio and Chernoray [26]	Underlying old roughness and poor application, epoxy primer	420	Cebeci and Bradshaw [12] see Eq. (2), C_s = 0.253	85	5

when it comes to prediction of additional resistance and nominal wake fraction, using a certain hull roughness model, has been evaluated for a few cases and observed to be minor.

Convergence is measured through average residuals as well as averaged quantities such as resistance. A simulation is considered converged when the residuals are stable and the resistance is deviating within ± 0.2% from its mean value.

5.1. Computational domain and boundary conditions

The CFD model of the KVLCC2 consists of a fixed hull without a rudder and with the free surface replaced by a symmetry plane (double-body simulations). Since the resistance of KVLCC2 is dominated by frictional resistance, it will give a relatively good picture of the relative differences between hull roughness models, and these simplifications reduce the required computational resources significantly.

The size of the computational domain given in [x, y, z] is [-3.5L_{PP}:2.5L_{PP}, 0:2L_{PP}, -1.5L_{PP}:0L_{PP}] ([0,0,0] located at mid-ship). A symmetry boundary condition is specified at the ship's centreline (y = 0) and only the half hull is included in the flow domain. An inlet velocity boundary condition is specified at the inlet and lateral boundaries. On the outlet, a uniform pressure is prescribed. Three operating conditions are simulated for each hull roughness model, corresponding to $Re_{L_{PP}} \sim 1.3$, 1.7 and $2.0 \cdot 10^9$ (corresponding to Fn = 0.1, 0.125 and 0.15), to be able to identify differences in Reynolds number dependency between the hull roughness models. Water properties for salt water at 10 °C are used.

For a reference case the hull surface is modelled as hydraulically smooth, for the other cases various roughness functions and associated roughness length scales are applied, according to specifications in Tables 2–4. The "all-y^+" wall treatment has been applied for all simulations, implying that a resolved viscous sublayer or the application of wall functions is applied dependent on the near-wall spacing. This is enabled in STAR-CCM+ through a blending function based on wall-distance Reynolds number [31]. Due to the near wall y^+ of the grids, see Section 5.2, the traditional wall function approach will be applied, in STAR-CCM+ formulated as:

$$u^+ = \frac{1}{\kappa}\ln(Ey^+), \tag{4}$$

where the default constants $\kappa = 0.42$ and $E = 9.0$ are used (corresponding to a smooth-wall log-law intercept $B = 5.23$). The default roughness function implemented in STAR-CCM+ v12.06 [31] is expressed according to Cebeci and Bradshaw [12] with $C_s = 0.253$, which implies that it follows the traditional Nikuradse curve [5]. However it is implemented in a generic form as:

$$\Delta U^+ = \begin{cases} 0 & k^+ \le k^+_{smooth} \\ \frac{1}{\kappa}\ln\left(B\left(\frac{k^+ - k^+_{smooth}}{k^+_{rough} - k^+_{smooth}}\right) + C_s k^+\right) \cdot \sin\left(\frac{\pi}{2}\frac{\ln(k^+ / k^+_{smooth})}{\ln(k^+_{rough} / k^+_{smooth})}\right) & k^+_{smooth} < k^+ \le k^+_{rough} \\ \frac{1}{\kappa}\ln(B + C_s k^+) & k^+ > k^+_{rough} \end{cases} \tag{5}$$

with the possibility to modify the constants B, C_s (in STAR-CCM+ denoted C), k^+_{smooth}, and k^+_{rough} (in STAR-CCM+ denoted R^+_{smooth} and R^+_{rough}). To obtain Colebrook/Grigson, i.e. Eq. (3), only the expression for the fully turbulent regime is required, implying that k^+_{smooth} and k^+_{rough} needs to be set small enough so they are always exceeded, and $B = C_s = 1$. The roughness function by Schultz and Flack [8,13] and Cebeci and Bradshaw [12] are implemented with the constants provided in association with Eq. (2).

5.2. Computational grid

The computational grid consist of cut-cells, created using the

Table 4
Selected surfaces covered with light slime layers.

Publication	Description	Roughness function	Roughness length scale, k [μm]
Schultz [22]	SPC TBT fouled, 1 mm slime layer	Colebrook/Grigson, Eq. (3)	110
Schultz [7]	(Deteriorated coating or) light slime	Schultz and Flack [8,13] see Eq. (2)	100
Leer-Andersen et al. [24]	Light biofouling (slime)	Colebrook/Grigson, Eq. (3)	5.18

Fig. 2. KVLCC2 hull without rudder.

Table 5
Main particulars of KVLCC2.

Length between perpendiculars, L_{PP} [m]	320
Draft, T [m]	20.8
Displacement, Δ [m^3]	312 622
Wetted surface area without rudder, S_W [m^2]	27 194
Block coefficient, C_b	0.8098
Propeller diameter, D_P [m]	9.86
Axial position of propeller (distance from aft perpend.) [m]	5.6

Trimmer mesher in STAR-CCM+ v12.06. Volumetric refinements are applied around the ship and wake in general, and specifically around the bow and stern. See Figs. 3 and 4 for the resulting mesh structure (Grid 2) around the bow and stern, respectively.

The grid is constructed based on knowledge from previous studies [36,37] and complemented with a minor grid sensitivity analysis were the reference cell size is varied according to Table 6. However, the size of the near wall prism layers are not modified in the wall normal direction to avoid changes in the boundary conditions provided by the wall functions. The sensitivity analysis is conducted at one operating point, corresponding to $Re_{L_{PP}} = 1.3{\cdot}10^9$, with one hull surface model "Deteriorated coating or light slime" [7] and a smooth hull for reference. The total resistance coefficient, $C_T (= R/\frac{1}{2}\rho V_a^2 S_W$, where R is the resistance force and V_a the ship speed), additional resistance due to hull roughness ΔC_T, and predicted nominal wake fraction for each grid are given in Table 6. The numerical uncertainty can be estimated using a Rickardson extrapolation, even if it is not strictly valid due to the unstructured grid. For C_T the numerical uncertainty for Grid 1 and 2 are $\approx$ 0.0% and 0.2%, respectively, when assuming the order of accuracy to be 2 which suits the data well. For ΔC_T and nominal wake fraction the scatter in the results precludes an estimation of the numerical uncertainty, however the variations between the grids are negligible (about $\pm$ 1%) in relation to other uncertainties associated to the roughness models. Grid 2 will be applied within this study, it reduces the required computational resources in relation to Grid 1, but has a slightly higher numerical uncertainty for C_T. However, the variables in focus, ΔC_T and nominal wake fraction, are only marginally influenced by these differences in grid refinement.

The near-wall resolution of the grids, constructed for the use of wall functions, are 25 prism layers with an expansion ratio of 1.2 and a total prism layer thickness corresponding to 0.43% of L_{PP}. This implies for the given operating conditions an average y^+ of 160–230, dependent on speed. y^+ significantly exceeds the maximal k^+, as required. A minor sensitivity analysis to the selection of near wall cell height has been conducted at the same operating point, $Re_{L_{PP}} = 1.3{\cdot}10^9$, and surface roughness model, "Deteriorated coating or light slime" [7], as above. The near wall cell height was modified through removing, respectively adding, two prism layers. Grid details, ΔC_T relative to a smooth hull and nominal wake fraction are included in Table 7. The influence of these variations in y^+ on the overall results (in terms of ΔC_T relative to a smooth hull and nominal wake fraction) are negligible.

6. Comparison and discussion

For the hydrodynamic design of a vessel and its propulsion system, the additional resistance due to hull roughness as well as effects on the ship hull wake field are critical. The impact on these results, arising from the selection of a roughness model and hull condition (Section 3), is presently assessed on the KVLCC2 hull.

6.1. Comparison of hull resistance

The KVLCC2 additional resistance due to hull roughness are presented in terms of ΔC_T for the double-body model in Figs. 5–7 and ΔC_T in relative terms towards a smooth hull in Tables 8–10. For comparison, ΔC_F obtained using the ITTC-78 performance prediction method [1], i.e. the correlation proposed by Townsin [38], are included. Despite its naming, ΔC_F, it is a measure of the added total resistance due to roughness and not just the added frictional resistance.

For the surfaces referred to as newly painted with high quality, Fig. 5 and Table 8, the range of predicted relative additional resistance at $Re_{L_{PP}} = 2.0{\cdot}10^9$ is comparatively narrow 0–4.3%, with an outlier at 7.2%. No clear correlation can however be noted between the provided AHR of each surface and its computed additional resistance for KVLCC2. This shows, as claimed in several previous studies within the field, the high dependency of resistance on surface texture, and maybe other properties such as hydrophobicity and surface elasticity, and not only roughness amplitude. The ITTC-78/Townsin correlation is developed based on 10 ships with roughness varying between 144 and

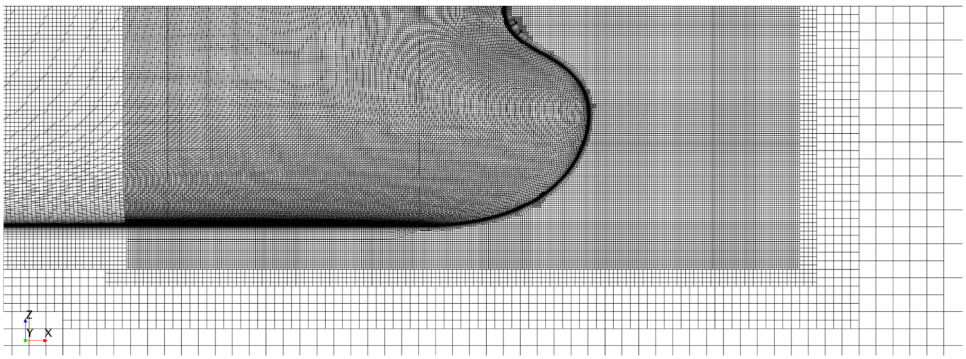

Fig. 3. Computational grid (Grid 2) at the hull and symmetry plane, showing refinements around the bow.

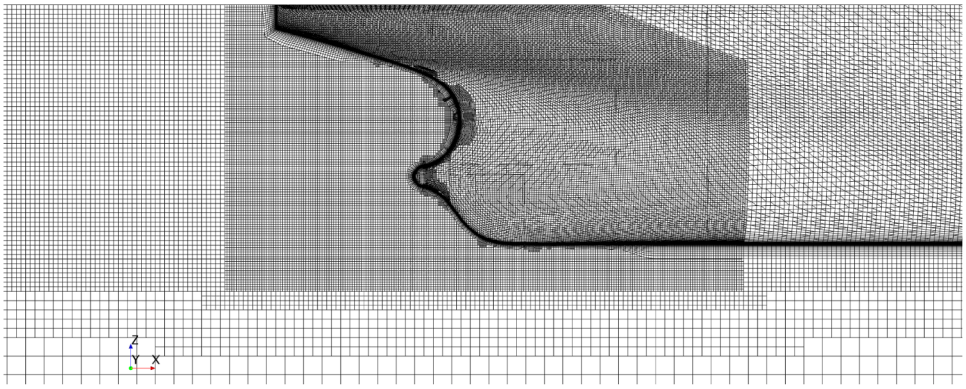

Fig. 4. Computational grid (Grid 2) at the hull and symmetry plane, showing refinements around the stern.

Table 6
Grid details and results for grid sensitivity analysis. Rough surface model according to "Deteriorated coating or light slime" [7] at $Re_{LPP} = 1.3{\cdot}10^9$.

	Grid 1	Grid 2	Grid 3	Grid 4	Grid 5
Number of cells	$24.4 \cdot 10^6$	$13.8 \cdot 10^6$	$7.9 \cdot 10^6$	$4.6 \cdot 10^6$	$1.7 \cdot 10^6$
cell size / cell size$_{[Grid\,1]}$	1	1.25	1.56	1.95	3.05
C_T	$2.117{\cdot}10^{-3}$	$2.121{\cdot}10^{-3}$	$2.124{\cdot}10^{-3}$	$2.128{\cdot}10^{-3}$	$2.140{\cdot}10^{-3}$
ΔC_T	$2.65{\cdot}10^{-4}$	$2.63{\cdot}10^{-4}$	$2.62{\cdot}10^{-4}$	$2.62{\cdot}10^{-4}$	$2.63{\cdot}10^{-4}$
Nominal wake fraction	0.345	0.345	0.348	0.344	0.340

Table 7
Grid details and results for sensitivity analysis to near wall cell height. Rough surface model according to "Deteriorated coating or light slime" [7] at $Re_{LPP} = 1.3{\cdot}10^9$.

	Grid 2, $y^+\downarrow$	Grid 2	Grid 2, $y^+\uparrow$
Number of cells	$14.1 \cdot 10^6$	$13.8 \cdot 10^6$	$13.5 \cdot 10^6$
Average y^+	112	162	234
ΔC_T relative to a smooth hull	14.16%	14.18%	14.24%
Nominal wake fraction	0.344	0.345	0.346

206 μm [39] and is therefore unsuitable to apply for such low values of AHR as listed in Table 8. Applying the Townsin correlation at, for instance, AHR = 70 μm would even appear as negative additional resistance at $Re_{LPP} = 1.3{\cdot}10^9$. The ITTC-78/Townsin correlation for AHR = 150 μm results in an additional resistance higher than the models included for newly painted surfaces with high quality, with the outlier excepted. Another question relevant for a CFD-user aiming to model a newly painted hull, is as previously discussed whether these surfaces are realistic on a real ship hull. For the experiments, the paint application is carried out in laboratory settings allowing a better control of both environmental factors and application technique compared to what usually is possible on a real ship hull. That this may be the case is also evident through the low AHR of the surfaces included in the review, in relation to AHR of new ships which commonly lies between 75–125 μm [25]. It may therefore be questioned whether it really is relevant to apply roughness models representing such smooth surfaces in CFD, even for newly painted ships. Finally, all surfaces referred to as newly painted with high quality, except from two, are modelled using the Colebrook/Grigson roughness function (Eq. (3)). It is clear that the roughness function by Schultz and Flack [8,13] implies a stronger dependency between ΔC_T and the Reynolds number of the flow (Fig. 5: Schultz 2007 [7]), as a result of a steeper, inflectional roughness function (Fig. 1 and Eq. (2)), which is closer to the ITTC-78/Townsin prediction.

For the second group, surfaces with different extent of poor paint application and/or hull coating damages (Fig. 6 and Table 9) the differences between the surfaces are wider, both in terms of how they are described and also in terms of provided AHR, in relation to the group of high quality ship hull surfaces discussed above. For the surfaces with poor paint application and/or hull coating damages a correlation between the impact on resistance and AHR can be observed, which ought to be expected due to the large differences between the surfaces, ranging from AHR of 110 μm to 420 μm. Also for these surface it seems reasonable that the surface texture, and maybe other properties such as

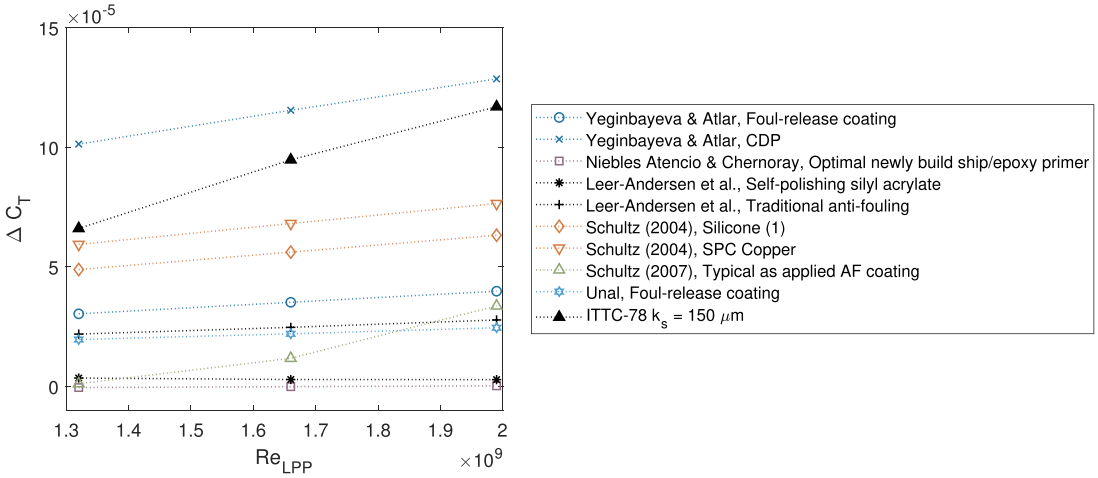

Fig. 5. Additional resistance (ΔC_T) as a function of Reynolds number based on L_{PP} for KVLCC2 with various models for high quality, newly painted surfaces.

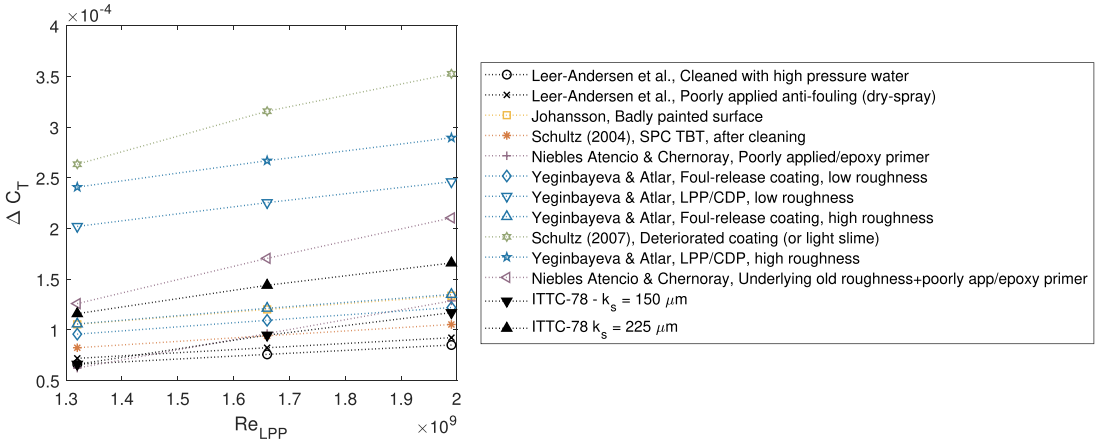

Fig. 6. Additional resistance (ΔC_T) as a function of Reynolds number based on L_{PP} for KVLCC2 with various models for surfaces with different extent of poor paint application and/or hull coating damages.

hydrophobicity and surface elasticity, are important for boundary layer development and resistance characteristics, and this is a possible explanation for the scatter in the correlation between AHR and ΔC_T. This is clearly exemplified in [25] where the Linear-polishing polymer/Controlled-depletion polymer and Foul-release coating, both with AHR $\sim$ 250, have a very different impact on ΔC_T, due to their surface characteristics. Foul-release coatings are mainly based on low modulus of elasticity, which implies that the coating changes its shape under load, with lower additional resistance of the unfouled surface as a positive consequence. The ITTC-78/Townsin prediction is included for AHR = 150 and 225 μm respectively, the latter value being in the upper range of AHR which this correlation is suitable for [39], and are in line with the general trend of the hull roughness models. This can be interpreted as if the ITTC-78/Townsin correlation still may be relevant for prediction of additional resistance, however it shall be kept in mind that the scatter due to surface texture and other properties is extensive, and neither will the influences on the wake field be represented using the correlation only. Finally, it is also observed for these surfaces that those associated with a roughness function of inflectional behavior, i.e. here either the one by Schultz and Flack [8,13] or by Cebeci and Bradshaw [12], imply a stronger dependency between ΔC_T and the Reynolds number of the flow (Fig. 6, Schultz [7] and Niebles Atencio and Chernoray [26]).

The third group, containing surfaces covered with light slime layers (Fig. 7 and Table 10), only includes three surfaces, but is still an indication of what has been observed in several previous studies; slime layers/biofilms are very difficult to characterize and there is a wide variability in their impact on hull resistance. The relative additional resistance at $Re_{L_{PP}} = 2.0 \cdot 10^9$ varies between 7.7 and 45.5%. Townsin [4] summarizes several studies on the fouling penalty of slime layers, with the impact on resistance ranging from 5 to 25% in relation to a clean hull. More recent studies by Schultz et al. [30] also includes an example of the change in required shaft power of a mid-sized naval surface combatant due to slime, with results ranging from 1.5% to 10.1% for various coverage of biofilms. The wide variability in the slime layers impact on hull resistance really poses a problem and imply uncertainties to the CFD-user since slime layers are frequently present on ship hulls.

6.2. Comparison of wake fields

In Table 11–13 the predicted KVLCC2 nominal wake fraction are included. The wake fields are evaluated at the propeller plane, specified according to Table 5. Further, the wake fields are shown as contour plots for a smooth hull, as well as three selected surfaces; “Traditional Anti-fouling” (high-quality application) [24], “Foul-release coating, high roughness” [25], and “Deteriorated coating or light slime” [7] in Fig. 8.

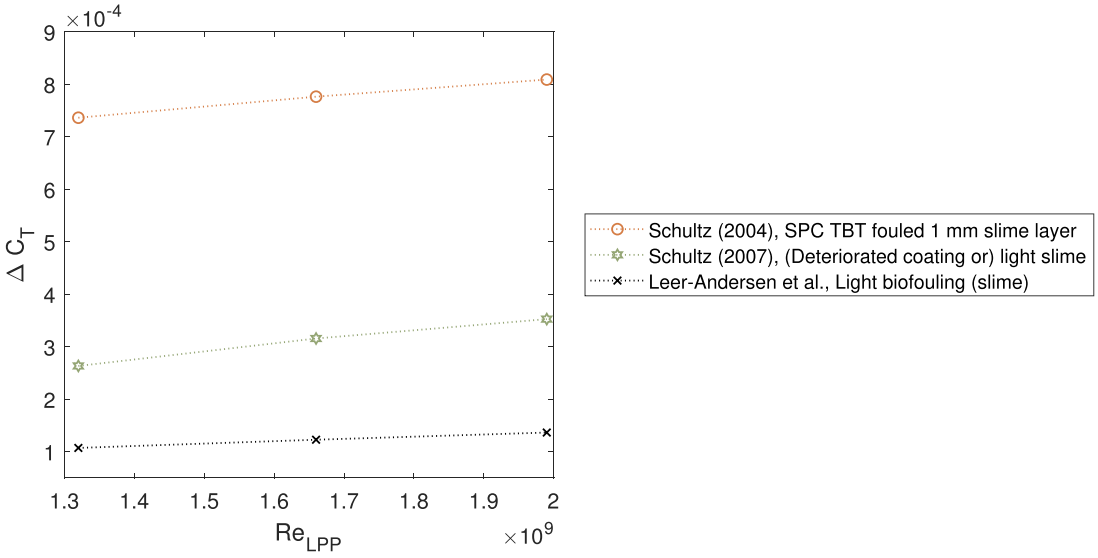

Fig. 7. Additional resistance (ΔC_T) as a function of Reynolds number based on L_{PP} for KVLCC2 with various models for surfaces covered with light slime layers.

Table 8
Relative additional resistance (ΔC_T) towards a smooth hull at $Re_{L_{PP}} = 2.0{\cdot}10^9$ ($Fn = 0.15$) for KVLCC2 with various models for high quality, newly painted surfaces.

Publication	Description	AHR [μm]	ΔC_T relative to a smooth hull
Yeginbayeva and Atlar [25]	Foul-release coating	~40	2.2%
Yeginbayeva and Atlar [25]	Controlled-depletion polymer (CDP)	~50	7.2%
Niebles Atencio and Chernoray [26]	Optimal newly build ship, epoxy primer	56	No resistance increase
Leer-Andersen et al. [24]	Self-polishing silyl acrylate	~65	0.2%
Leer-Andersen et al. [24]	Traditional anti-fouling	~65	1.6%
Schultz [22]	Silicone (1)	66	3.6%
Schultz [22]	SPC Copper	97	4.3%
Schultz [7]	Typical as applied AF coating	150	1.9%
Ünal [23]	Foul-release coating	-	1.4%
	ITTC-78/Townsin [38]	150	6.6%

Table 9
Relative additional resistance (ΔC_T) towards a smooth hull at $Re_{L_{PP}} = 2.0{\cdot}10^9$ ($Fn = 0.15$) for KVLCC2 with various models for surfaces with different extent of poor paint application and/or hull coating damages.

Publication	Description	AHR [μm]	ΔC_T relative to a smooth hull
Leer-Andersen et al. [24]	Cleaned with high pressure water	~110	4.8%
Leer-Andersen et al. [24]	Poorly applied anti-fouling (dry-spray)	~130	5.2%
Johansson [21]	Badly painted surface	132	7.5%
Schultz [22]	SPC TBT, after cleaning	135	5.9%
Niebles Atencio and Chernoray [26]	Poorly applied coating, epoxy primer	214	7.2%
Yeginbayeva and Atlar [25]	Foul-release coating, low roughness	~220	6.9%
Yeginbayeva and Atlar [25]	Linear-polishing polymer (LPP)/ Controlled-depletion polymer (CDP), low roughness	~250	13.9%
Yeginbayeva and Atlar [25]	Foul-release coating, high roughness	~250	7.6%
Schultz [7]	Deteriorated coating (or light slime)	300	19.8%
Yeginbayeva and Atlar [25]	Linear-polishing polymer (LPP)/ Controlled-depletion polymer (CDP), high roughness	~320	16.3%
Niebles Atencio and Chernoray [26]	Underlying old roughness and poor application, epoxy primer	420	11.8%
	ITTC-78/Townsin [38]	150	6.6%
	ITTC-78/Townsin [38]	225	9.4%

Table 10
Relative additional resistance (ΔC_T) towards a smooth hull at $Re_{L_{PP}} = 2.0{\cdot}10^9$ ($Fn = 0.15$) for KVLCC2 with various models for surfaces covered with light slime layers.

Publication	Description	ΔC_T relative to a smooth hull
Schultz [22]	SPC TBT fouled, 1 mm slime layer	45.5%
Schultz [7]	(Deteriorated coating or) light slime	19.8%
Leer-Andersen et al. [24]	Light biofouling (slime)	7.7%

Table 11
Predicted nominal wake fraction at $Re_{L_{PP}} = 2.0{\cdot}10^9$ ($Fn = 0.15$) for KVLCC2 with various models for high quality, newly painted surfaces.

Publication	Description	AHR [μm]	Nominal wake fraction
Yeginbayeva and Atlar [25]	Foul-release coating	~40	0.314
Yeginbayeva and Atlar [25]	Controlled-depletion polymer (CDP)	~50	0.323
Niebles Atencio and Chernoray [26]	Optimal newly build ship, epoxy primer	56	0.310
Leer-Andersen et al. [24]	Self-polishing silyl acrylate	~65	0.310
Leer-Andersen et al. [24]	Traditional anti-fouling	~65	0.312
Schultz [22]	Silicone (1)	66	0.317
Schultz [22]	SPC Copper	97	0.318
Schultz [7]	Typical as applied AF coating	150	0.312
Ünal [23]	Foul-release coating	-	0.312
	Smooth hull	N/A	0.310

The relative changes in predicted nominal wake fraction for the newly painted surfaces are 0–4.2%, for the surfaces with different extent of poor paint application and/or hull coating damages 2.6–11.6%, and for the surfaces covered with light slime layers 4.5–28.4%. These results seems reasonable in relation to other studies focusing on the surface roughness influence on nominal wake fraction [40,41]. However, proper flow field validation in ship-scale is dependent on future developments/research on ship-scale measurements, the same holds for validation on how the CFD models predict roughness effects on flow separation in ship-scale. As previously noted, all roughness models are based on experiments conducted on flat plates without any pressure gradients in the flow, unlike the flow around curved ship hull surfaces. In Fig. 8 the thicker boundary layers due to hull roughness are notable. The impact on the wake field is seen through both higher wake peaks and more evident bilge vortices with increasing roughness.

7. Conclusions

The review of existing methods to model hull roughness shows the use of a variety of roughness functions, both Colebrook-type and

Table 12
Predicted nominal wake fraction at $Re_{L_{PP}} = 2.0{\cdot}10^9$ ($Fn = 0.15$) for KVLCC2 with various models for surfaces with different extent of poor paint application and/or hull coating damages.

Publication	Description	AHR [μm]	Nominal wake fraction
Leer-Andersen et al. [24]	Cleaned with high pressure water	~110	0.318
Leer-Andersen et al. [24]	Poorly applied anti-fouling (dry-spray)	~130	0.319
Johansson [21]	Badly painted surface	132	0.323
Schultz [22]	SPC TBT, after cleaning	135	0.320
Niebles Atencio and Chernoray [26]	Poorly applied coating, epoxy primer	214	0.322
Yeginbayeva and Atlar [25]	Foul-release coating, low roughness	~220	0.322
Yeginbayeva and Atlar [25]	Linear-polishing polymer (LPP)/ Controlled-depletion polymer (CDP), low roughness	~250	0.336
Yeginbayeva and Atlar [25]	Foul-release coating, high roughness	~250	0.324
Schultz [7]	Deteriorated coating (or light slime)	300	0.346
Yeginbayeva and Atlar [25]	Linear-polishing polymer (LPP)/ Controlled-depletion polymer (CDP), high roughness	~320	0.340
Niebles Atencio and Chernoray [26]	Underlying old roughness and poor application, epoxy primer	420	0.331
	Smooth hull	N/A	0.310

Table 13
Predicted nominal wake fraction at $Re_{L_{PP}} = 2.0{\cdot}10^9$ ($Fn = 0.15$) for KVLCC2 with various models for surfaces covered with light slime layers.

Publication	Description	Nominal wake fraction
Schultz [22]	SPC TBT fouled, 1 mm slime layer	0.398
Schultz [7]	(Deteriorated coating or) light slime	0.346
Leer-Andersen et al. [24]	Light biofouling (slime)	0.324
	Smooth hull	0.310

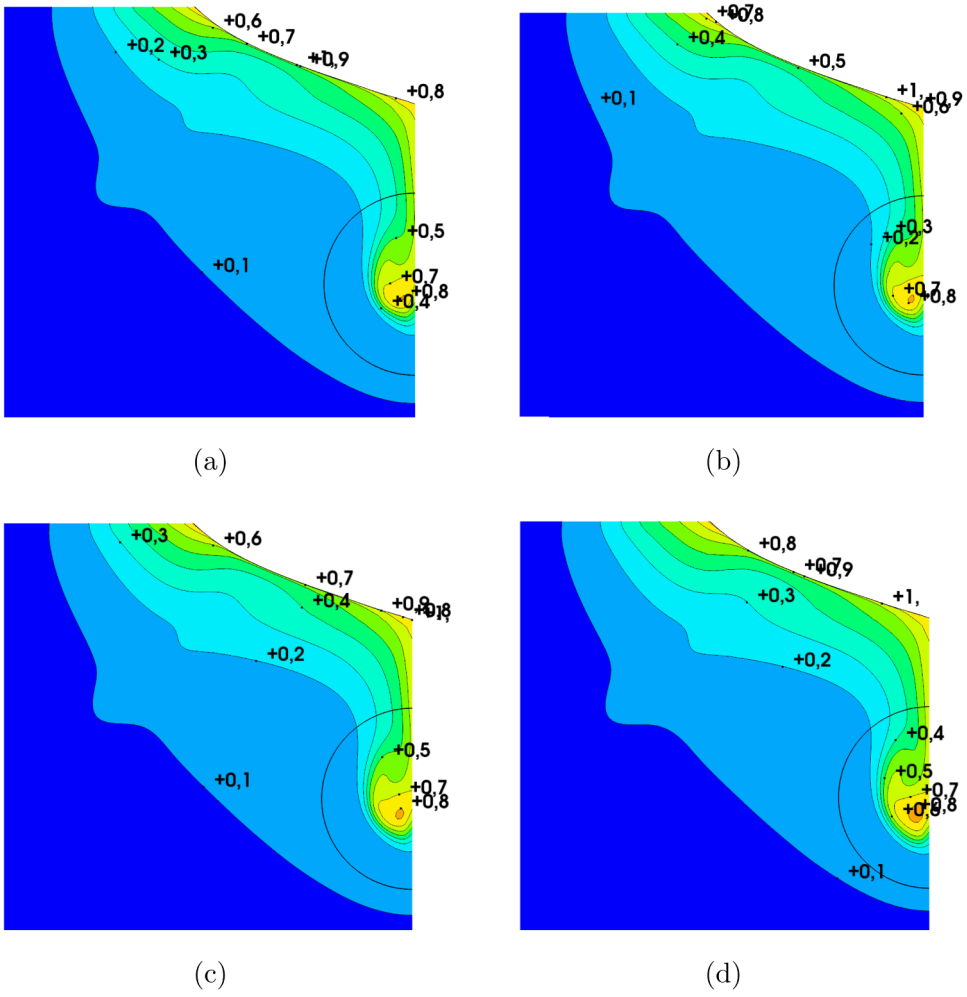

Fig. 8. Contour plot of wake fraction at the KVLCC2 propeller plane at $Re_{L_{PP}} = 2.0{\cdot}10^9$ ($Fn = 0.15$). for: (a) Smooth hull, (b) "Traditional Anti-fouling" (high-quality application) [24], (c) "Foul-release coating, high roughness" [25], and (d) "Deteriorated coating or light slime" [7].

inflectional with three distinct flow regimes, as well as a variety of strategies to obtain the roughness length scales. We have not within this review noted any convergence within the research community towards specific roughness functions or methods to obtain the roughness length scales.

The comparison of different methods to model hull roughness shows a moderate correlation between additional resistance and AHR, with large scatter due to differences in surface texture, and maybe other properties such as hydrophobicity and surface elasticity, for surfaces with different extent of poor paint application and/or hull coating damages. Amongst the models for high quality, newly painted surfaces no clear correlation between additional resistance and AHR can be noted. Further, for slime layers/biofilms, similar conclusions as drawn in previous studies can be made here; they are very difficult to characterize and there is a wide variability in their impact on hull resistance. These observations implies that to be able to select a proper model for hull roughness for a CFD-setup the surface needs to be characterised in more detail, including type of hull coating and details of possible fouling, and not only through AHR which traditionally has been considered for the ITTC-78/Townsin correlation. Consequently, if no study is published for similar conditions, the surface roughness influence on the boundary layer is preferably evaluated, using any of the experimental methods applied in the studies referred to in this review.

As noted within the review it can be problematic to compare different hull roughness models and surfaces referred to in the studies since the detailed surface parameters often used are dependent on measurement technique and filtering of data for which there is no standardized method. To facilitate comparison, transfer of knowledge between studies, and usage of the results within a wider group, it would be beneficial if the research community agreed upon a standardized procedure to obtain a few specific more detailed surface parameters.

Not included within this study is the possible influence on the boundary layer, and hence additional resistance, of other surface imperfections such as weld seams, anodes, larger surface damages, plate dents etc. This could be studied further for more general cases, but is still a modelling assumption that needs to be considered for each ship-scale CFD-setup.

Future studies on hull roughness effects on ship-scale resistance and nominal wakes, as well as self-propulsion conditions, should consider using a range of roughness length scales representative of expected range of in-service conditions. These conditions would at least include two extremes: 1) the best achievable new-built coating application; and 2) a more realistic in-service condition, i.e. a moderate-to-heavy slime, possibly in combination with hull roughness and other surface imperfections. Detailed flow data at ship-scale would be invaluable for the development and validation of hull roughness modelling.

CRediT authorship contribution statement

Jennie Andersson: Conceptualization, Methodology, Validation, Formal analysis, Investigation, Writing - original draft, Visualization, Project administration. **Dinis Reis Oliveira:** Conceptualization, Methodology, Formal analysis, Resources, Writing - review & editing. **Irma Yeginbayeva:** Conceptualization, Methodology, Formal analysis, Resources, Writing - review & editing. **Michael Leer-Andersen:** Formal analysis, Resources, Writing - review & editing. **Rickard E. Bensow:** Conceptualization, Methodology, Formal analysis, Writing - review & editing, Supervision, Funding acquisition.

Declaration of Competing Interest

The authors declare that they have no known competing financial interests or personal relationships that could have appeared to influence the work reported in this paper.

Acknowledgements

This research is supported by the Swedish Energy Agency (grant number 38849-1 and 38849-2), the Swedish Transport Administration (grant number TRV 2018/76560) and Kongsberg Maritime Sweden through the University Technology Centre in Computational Hydrodynamics hosted by the Department of Mechanics and Maritime Sciences at Chalmers. The simulations were performed on resources at Chalmers Centre for Computational Science and Engineering (C3SE) and National Supercomputer Centre in Sweden (NSC), both provided by the Swedish National Infrastructure for Computing (SNIC).

References

[1] ITTC, 1978 ITTC Performance Prediction Method. Recommended Procedure 7.5 - 02 - 03 - 01.4 Rev 04, 2017.
[2] L. Larsson, F. Stern, M. Visonneau, Numerical Ship Hydrodynamics An assessment of the Gothenburg 2010 Workshop, Springer, Dordrecht, 2014.
[3] L. Larsson, F. Stern, M. Visonneau, T. Hino, N. Hirata, J. Kim, Proceedings, Tokyo 2015 Workshop on CFD in Ship Hydrodynamics, 2015.
[4] R.L. Townsin, The ship hull fouling penalty, Biofouling 19 (SUPPL.) (2003) 9–15.
[5] J. Nikuradse, Laws of Flow in Rough Pipes, NACA Technical Memorandum 1292, Technical Report, (1933).
[6] C.F. Colebrook, Turbulent flow in pipes, with particular reference to the transitional region between smooth and rough wall laws, J. Inst Civ. Eng. 11 (1939) 133–156.
[7] M.P. Schultz, Effects of coating roughness and biofouling on ship resistance and powering, Biofouling 23 (5) (2007) 331–341.
[8] Y.K. Demirel, O. Turan, A. Incecik, Predicting the effect of biofouling on ship resistance using CFD, Appl. Ocean Res. 62 (2017) 100–118.
[9] D.M. Yebra, S. Kiil, K. Dam-Johansen, Antifouling technology - past, present and future steps towards efficient and environmentally friendly antifouling coatings, Prog. Org. Coat. 50 (2004) 75–104.
[10] D. Ponkratov, Proceedings of 2016 Workshop on Ship Scale Hydrodynamic Computer Simulation, 2017.
[11] N. Speranza, B. Kidd, M.P. Schultz, I.M. Viola, Modelling of hull roughness, Ocean Eng. 174 (2019) 31–42.
[12] T. Cebeci, P. Bradshaw, Momentum Transfer in Boundary Layers, Hemisphere Publishing/McGraw-Hill, 1977.
[13] M.P. Schultz, K.A. Flack, The rough-wall turbulent boundary layer from the hydraulically smooth to the fully rough regime, J. Fluid Mech. 580 (2007) 381–405.
[14] K.A. Flack, M.P. Schultz, W.B. Rose, The onset of roughness effects in the transitionally rough regime, Int. J. Heat Fluid Flow 35 (2012) 160–167.
[15] C. Grigson, Drag losses of new ships caused by hull finish, J. Ship Res. 36 (2) (1992) 182–196.
[16] ITTC, Report of The Resistance and Flow Committee (19th ITTC), Technical Report, (1990).
[17] D.C. Wilcox, Turbulence Modelling for CFD, third ed., DCW Industries, 2006.
[18] L. Eça, M. Hoekstra, H.C. Raven, Quantifying roughness effects by ship viscous flow calculations, 28th Symposium on Naval Hydrodynamics, Pasadena, California, USA, (2010).
[19] B. Aupoix, Wall roughness modelling with k-ω SST Model, 10th International ERCOFTAC Symposium on Engineering Turbulence Modelling and Measurements, Marbella, Spain, (2014).
[20] M. Candries, Drag and Boundary Layer on Antifouling Paint, University of Newcastle-Upon Tyne, UK, 2001 Ph.D. thesis.
[21] L.-E. Johansson, The local effect of hull roughness on skin friction. Calculations based on floating element data and three-dimensional boundary layer theory, RINA Transactions, London, United Kingdom, (1984), pp. 187–201.
[22] M.P. Schultz, Frictional resistance of antifouling coating systems, J. Fluids Eng. 126 (6 (2004)) (2004).
[23] U.O. Ünal, Correlation of frictional drag and roughness length scale for transitionally and fully rough turbulent boundary layers, Ocean Eng. 107 (2015) 283–298.
[24] M. Leer-Andersen, S. Werner, K. Kim, Slutrapport för “Ytfriktionsdatabas for maritima sektorn”, Technical Report, Göteborg, Sweden, 2018.
[25] I.A. Yeginbayeva, M. Atlar, An experimental investigation into the surface and hydrodynamic characteristics of marine coatings with mimicked hull roughness ranges, Biofouling 34 (9) (2018) 1001–1019.
[26] B. Niebles Atencio, V. Chernoray, A resolved RANS CFD approach for drag characterization of antifouling paints, Ocean Eng. 171 (2019) 519–532.
[27] L. Savio, B.O. Berge, K. Koushan, M. Axelsson, Measurements of added resistance due to increased roughness on flat plates, AMT, Istanbul, Turkey, (2015).
[28] M. Leer-Andersen, Skin friction database, 2018, https://www.sspa.se/tools-and-methods/skin-friction-database.
[29] M.P. Schultz, G.W. Swain, The effect of biofilms on turbulent boundary layers, J. Fluids Eng. 121 (1999) 44–51.
[30] M.P. Schultz, J.M. Walker, C.N. Steppe, K.A. Flack, Impact of diatomaceous biofilms on the frictional drag of fouling-release coatings, Biofouling 31 (9) (2015) 759–773.
[31] S.P. Software, STAR-CCM+ Documentation version 12.06, 2017.
[32] F.R. Menter, Two-equation eddy-viscosity turbulence models for engineering applications, AIAA J. 32 (8) (1994) 1598–1605.

[33] F.R. Menter, M. Kuntz, R. Langtry, Ten years of industrial experience with the SST turbulence model, in: K. Hanjalic, Y. Nagano, M. Tummers (Eds.), Turbulence, Heat and Mass Transfer 4, Begell House, Inc., 2003.
[34] P.R. Spalart, Strategies for turbulence modelling and simulations, Int. J. Heat Fluid Flow 21 (3) (2000) 252–263.
[35] S.K. Arolla, P.A. Durbin, Modeling rotation and curvature effects within scalar eddy viscosity model framework, Int. J. Heat Fluid Flow 39 (2013) 78–89.
[36] J. Andersson, M. Hyensjö, A. Eslamdoost, R.E. Bensow, CFD Simulations of the Japan bulk carrier test case, Proceedings of the 18th Numerical Towing Tank Symposium, Cortona, Italy, (2015).
[37] J. Andersson, R. Gustafsson, A. Eslamdoost, R.E. Bensow, On the selection of optimal propeller diameter for a 120 m cargo vessel, SNAME Propeller-Shafting 2018 Symposium, Norfolk, Virginia, USA, (2018).
[38] R.L. Townsin, The ITTC Line - it's genesis and correlation allowance, The Naval Architect, RINA, (1985), pp. E359–E362.
[39] R.L. Townsin, S.K. Dey, The correlation of roughness drag with surface characteristics, Marine Roughness and Drag workshop, RINA, London, United Kingdom, (1990).
[40] T. Guiard, S. Leonard, F. Mewis, The Becker Mewis duct - challenges in full-scale design and new developments for fast ships, Proceedings of the Third International Symposium on Marine Propulsors, Launceston, Tasmania, Austrailia, (2013).
[41] S. Song, Y.K. Demirel, M. Atlar, An investigation into the effect of biofouling on the ship hydrodynamic characteristics using CFD, Ocean Eng. 175 (2019) 122–137.